Oxidation of DNA and RNA by Oxoruthenium(IV) Metallointercalators: Visualizing the Recognition Properties of Dipyridophenazine by High-Resolution Electrophoresis

Pamela J. Carter, Chien-Chung Cheng, and H. Holden Thorp*

Contribution from the Department of Chemistry, University of North Carolina, Chapel Hill, North Carolina 27599-3290

Received August 22, 1997

Abstract: The binding specificity for the intercalating Ru(tpy)(dppz)O^{2+} complex (tpy = 2,2′,2″-terpyridine; dppz = dipyridophenazine) was investigated for duplex DNA, HIV-1 TAR DNA and RNA, and $tRNA^{Phe}$. Unlike other dppz compounds studied to date, this compound cleaves nucleic acids at short range, and the resulting cleavage pattern can therefore be directly related to the recognition properties of the dppz ligand. To assign the intercalative recognition sites, a comparison was first made between the cleavage patterns of Ru(tpy)(dppz)O^{2+} and Ru(tpy)(bpy)O^{2+} (bpy = 2,2′-bipyridine), which differs from Ru(tpy)(dppz)O^{2+} only by the absence of the intercalative dppz functionality. Cleavage sites common to both complexes were assigned to binding properties other than intercalation, whereas any additional sites observed for Ru(tpy)(dppz)O^{2+} were strongly implicated as the sites of intercalative recognition. It was necessary, however, to distinguish between those sites which represent a strong binding affinity and those sites which were instead made more accessible to cleavage by binding of another equivalent of the intercalating complex at a remote site. We therefore investigated the cleavage pattern of Ru(tpy)(bpy)O^{2+} with and without the classical intercalator Pt(tpy)$(HET)^{+}$ (HET = 2-hydroxyethanethiolate) to determine the effect of decoupling the intercalative recognition and oxidation chemistry. In this experiment, sites where cleavage inhibition was observed were indicative of intercalative recognition by the platinum complex, whereas sites where cleavage enhancement was observed strongly suggested that intercalative binding at a remote site had altered the structure of the nucleic acid. Comparison of the cleavage patterns of Ru(tpy)(bpy)O^{2+} and Ru(tpy)(dppz)O^{2+} for a duplex oligonucleotides, tRNA, and stem−loop structures suggests a recognition pattern for the dppz ligand very similar to that of classical intercalators.

Introduction

The binding and recognition of DNA by metal complexes of dipyridophenazine (dppz) is an area of intense interest[1−4] that stems in part from the discovery that complexes based on Ru(bpy)$_2$(dppz)$^{2+}$ exhibit long-lived emission when intercalated into duplex DNA but not when free in solution, which has been referred to as the "molecular light switch" effect (bpy = 2,2′-bipyridine).[3,5] These complexes have also been used to study electron transfer through the stacked bases of duplex DNA, because these moieties offer an intercalated, long-lived excited state that can participate in electron-transfer reactions.[6,7] Although numerous experiments support an intercalative binding mode,[1−4] there is little information on the sequence specificity of binding of octahedral dppz complexes. NMR experiments on a hexamer duplex implicate binding of Ru(phen)$_2$(dppz)$^{2+}$ in the major groove in two binding modes;[8] however, the broad sequence and structure preferences of the complex could not be assessed within the context of a small oligonucleotide.

We report here on the complex Ru(tpy)(dppz)O^{2+}, which combines the intercalative dppz ligand with a reactive oxoruthenium(IV) functionality that cleaves DNA by oxidation of guanine and the 1′ deoxyribose hydrogen (Scheme 1, tpy = 2,2′,2″-terpyridine). These studies provide the first opportunity to use high-resolution electrophoresis to elucidate binding specificity of the dppz ligand; this approach has been extraordinarily successful in studies of recognition of the related phenanthrenequinone diimine (phi) ligand,[9,10] and the value of such experiments in a dppz system has been discussed.[8] In the studies described here, the Ru(tpy)(dppz)O^{2+} complex can be compared with Ru(tpy)(bpy)O^{2+}, which differs only by the absence of the intercalating dppz functionality; sites unique to Ru(tpy)(dppz)O^{2+} are therefore strongly implicated as resulting from preferential recognition by the dppz ligand. The Ru(tpy)(bpy)O^{2+} complex does contain the tpy ligand, which is known to lead to intercalation of square planar complexes;[11,12] however, intercalation of octahedral complexes containing tpy is sterically

(1) Neyhart, G. A.; Grover, N.; Smith, S. R.; Kalsbeck, W. A.; Fairley, T. A.; Cory, M.; Thorp, H. H. *J. Am. Chem. Soc.* **1993**, *115*, 4423−4428.
(2) Hiort, C.; Lincoln, P.; Nordén, B. *J. Am. Chem. Soc.* **1993**, *115*, 3448−3454.
(3) Jenkins, Y.; Friedman, A. E.; Turro, N. J.; Barton, J. K. *Biochemistry* **1992**, *31*, 10809−10816.
(4) Stoeffler, H. D.; Thornton, N. B.; Temkin, S. L.; Schanze, K. S. *J. Am. Chem. Soc.* **1995**, *117*, 7119−7128.
(5) Friedman, A. E.; Chambron, J. C.; Sauvage, J. P.; Turro, N. J.; Barton, J. K. *J. Am. Chem. Soc.* **1990**, *112*, 4960−4962.
(6) Arkin, M. R.; Stemp, E. D. A.; Holmlin, R. E.; Barton, J. K.; Hoermann, A.; Oslon, E. J. C.; Barbara, P. F. *Science* **1996**, *273*, 475−480.
(7) Stemp, E. D. A.; Arkin, M. R.; Barton, J. K. *J. Am. Chem. Soc.* **1997**, *119*, 2921−2925.
(8) Dupureur, C. M.; Barton, J. K. *Inorg. Chem.* **1997**, *36*, 33−43.
(9) Pyle, A. M.; Long, E. C.; Barton, J. K. *J. Am. Chem. Soc.* **1989**, *111*, 4520−4522.
(10) Sitlani, A.; Long, E. C.; Pyle, A. M.; Barton, J. K. *J. Am. Chem. Soc.* **1992**, *114*, 2303−2312.

S0002-7863(97)02958-2 CCC: $15.00
Published on Web 01/16/1998

Scheme 1

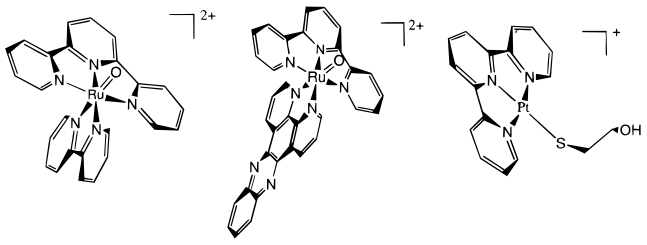

Ru(tpy)(bpy)O^{2+} **Ru(tpy)(dppz)O^{2+}** **Pt(tpy)(HET)$^{+}$**

precluded, which we have conclusively demonstrated in this particular case by showing that the parent Ru(tpy)(bpy)OH_2^{2+} complex does not lengthen DNA in a viscometry assay.[1] Oxidation of single-stranded, duplex, and bulge−loop DNA and bulge−loop and transfer RNA by Ru(tpy)(dppz)O^{2+} and Ru(tpy)(bpy)O^{2+} provide strong evidence that the dppz ligand imparts a selectivity for favorable intercalation sites and that the complex is bound at least in part in the minor groove. These conclusions are supported by experiments on Ru(tpy)(bpy)O^{2+} in conjunction with the exogenous intercalator Pt(tpy)$(HET)^{+}$, which independently demonstrate that the putative sites of intercalative recognition by Ru(tpy)(dppz)O^{2+} are also targeted by the known classical intercalator (HET = 2-hydroxyethanethiolate).[11,12] Furthermore, this unique comparison between Pt(tpy)$(HET)^{+}$ and Ru(tpy)(dppz)O^{2+} also allows us to distinguish between those sites affected by intercalative recognition and those affected by a structural change brought on by intercalation at another site. Taken together, the results show that the dppz complex recognizes well-established sites of intercalative binding, and this intercalation affects the structures of both TAR RNA and semidenatured tRNA but not TAR DNA. These experiments provide a way of assessing the tolerance of a given structure to intercalation at single-nucleotide resolution for complex nucleic acids.

Experimental Section

Metal Complexes. The complexes [Ru(tpy)(bpy)OH_2]$(ClO_4)_2$, [Ru(tpy)(dppz)OH_2]$(ClO_4)_2$, and [Pt(tpy)(HET)](ClO_4) were prepared according to published procedures.[12−14] The oxoruthenium(IV) complexes were prepared by electrochemical oxidation of the corresponding aquaruthenium(II) complexes in 10 mM sodium phosphate buffer (pH 7.0) as described previously.[1] Bulk electrolysis was performed at 0.85 V (vs Ag/AgCl) until the current reached 8% of the initial value.

DNA and RNA Preparation. Synthetic oligonucleotides were obtained from the Oligonucleotide Synthesis Center in the Department of Pathology at UNC. The DNA was purified by UV shadowing, as described previously.[15] The DNA concentrations were determined from the absorbance at 260 nm and are given on a per strand basis. The 5′-^{32}P-labeled oligomer was prepared by using T4 polynucleotide kinase and deoxyadenosine 5′-[γ-^{32}P]-triphosphate. The labeled DNA was isolated by ultracentrifugation using Centricon-10 filters (Amicon), as described previously.[15] To ensure hairpin formation, both the DNA and RNA were annealed in 10 mM sodium phosphate (pH 7.0) by heating to 90 °C for 3 min and cooling rapidly on ice to prevent the formation of dimers. The annealing conditions were then checked by running a native gel.

The TAR RNA was synthesized enzymatically using T7 RNA polymerase from a synthetic DNA template.[16] An extra GC base pair was added at the 5′ end to facilitate the transcription reaction. The RNA was purified by the UV-shadowing method and 3′-end-labeled using T4 RNA ligase and cytidine 3′,5′-[5′-^{32}P] diphosphate at 5 °C for 16 h.[17] The radiolabeled RNA was purified on a 20% denaturing gel (8 M urea). The gel pieces containing the labeled RNA were crushed and gently shaken for 2−3 h in a soaking solution (0.5 M ammonium acetate, 0.1% SDS, 0.1 M EDTA, pH 6) and were then filtered using a micropure 0.45 M separator (Amicon) to remove the acrylamide. Finally, ethanol precipitation was performed to recover the labeled RNA.

tRNA^{Phe}. Carrier tRNA and yeast tRNA^{Phe} (Sigma) were purified by dissolving in 0.3 M sodium acetate, 10 mM Tris-HCl (pH 7.5), 10 mM EDTA, and 0.5% SDS, extracted several times with phenol−chloroform, and recovered by ethanol precipitation. The 3′-end-labeled tRNA^{Phe} was prepared as described above and renatured by heating a 10 μL solution containing 5 μg carrier tRNA, 10 mM sodium phosphate (pH 7.0), 10 mM $MgCl_2$, and ^{32}P− tRNA^{Phe} (30−35000 cpm) at 50 °C for 8 min and cooling slowly to room temperature for 1 h. The presence of Mg^{2+} allows the tRNA to fold into its native form. Semidenatured tRNA was prepared by heating (50 °C, 8 min) the tRNA solution without $MgCl_2$ and immediately cooling it on ice.

Cleavage Reactions. The freshly oxidized Ru(tpy)(bpy)O^{2+} and Ru(tpy)(dppz)O^{2+} complexes were added to the DNA or RNA solution containing 10 mM sodium phosphate buffer (pH 7.0), ∼3nCi of labeled DNA or RNA, and 0.5 μg carrier tRNA for the TAR RNA cleavage reactions, 5 μg carrier tRNA for the tRNA^{Phe} reactions, or 5 μM unlabeled oligonucleotide for the DNA reactions. The solution conditions for tRNA^{Phe} are described above. The reactions were allowed to react for 5 min and were then quenched by adding 10 μL ethanol. Because a higher concentration of metal complex was required to oxidize tRNA^{Phe}, the reaction samples were ethanol precipitated to remove excess salt. Lyophilized pellets were then treated with base to convert all of the lesions to strand scission products. The DNA was treated with piperidine in a procedure that has been described elsewhere.[18] The piperidine reactions were carried out at 90 °C, which should disrupt any secondary structure and therefore dramatically reduces the possibility that the pattern of piperidine-labile cleavages is a result of the kinetics of hydrolysis rather than oxidation. Further, the results were identical with greater piperidine concentrations or reaction times, suggesting that all of the piperidine-labile lesions were converted to strand breaks. The RNA samples were treated with aniline (1.0 M aniline−acetate, pH 4.5).[19] This situation is somewhat different from the piperidine treatment of DNA, because at sufficient reaction times, hydrolysis of the undamaged RNA is detected. The conditions were such that the maximum amount of aniline-labile oxidation was observed above background hydrolysis of the undamaged RNA, again minimizing the chance that incomplete hydrolysis of oxidized lesions produces the observed sequence specificity.

The cleavage fragments were separated on a 20% denaturing (8 M urea) polyacrylamide gel (19:1 acrylamide: bis acrylamide). Sequencing reactions were performed by known chemical procedures.[19,20] Quantitation of the extent of cleavage was performed by integration of the optical density as a function of the band area using an Apple OneScanner and the Image program from the NIH. Care was taken to avoid saturation of the film so that only Gaussian peaks were observed during quantitation.

For experiments involving Pt(tpy)$(SCH_2CH_2OH)^{+}$, an increasing concentration of the exogenous metallointercalator was added to solutions containing 10 mM sodium phosphate (pH 7.0), carrier tRNA (0.5 μg) or cold DNA (5 μM), and ∼3 nCi of labeled DNA or RNA.

(11) Wang, A. H. J.; Nathans, J.; van der Mercel, G.; van Boom, J. H.; Rich, A. *Nature* **1978**, *276*, 471−474.
(12) Jennette, K. W.; Lippard, S. J.; Vassiliades, G. A.; Bauer, W. R. *Proc. Natl. Acad. Sci. U.S.A.* **1974**, *71*, 3839−3843.
(13) Takeuchi, K. J.; Thompson, M. S.; Pipes, D. W.; Meyer, T. J. *Inorg. Chem.* **1984**, *23*, 4, 1845−1851.
(14) Gupta, N.; Grover, N.; Neyhart, G. A.; Liang, W.; Singh, P.; Thorp, H. H. *Agnew. Chem., Int. Ed. Engl.* **1992**, *31*, 1048--1050.
(15) Carter, P. J.; Cheng, C.-C.; Thorp, H. H. *Inorg. Chem.* **1996**, *35*, 3348−3354.
(16) Milligan, J. F.; Groebe, D. R.; Witherell, G. W.; Uhlenbeck, O. C. *Nucleic Acids Res.* **1987**, *15*, 8783−8788.
(17) Bruce, A. G.; Uhlenbeck, O. C. *Nucleic Acids Res.* **1978**, *4*, 3665−3677.
(18) Cheng, C.-C.; Goll, J. G.; Neyhart, G. A.; Welch, T. W.; Singh, P.; Thorp, H. H. *J. Am. Chem. Soc.* **1995**, *117*, 2970−2980.
(19) Peattie, D. A. *Proc. Natl. Acad. Sci. U.S.A.* **1979**, *76*, 1760−1764.
(20) Maxam, A. M.; Gilbert, W. *Proc. Natl. Acad. Sci. U.S.A.* **1977**, *74*, 499−560.

Scheme 2

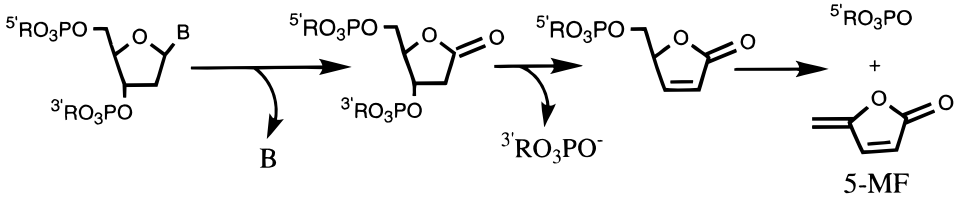

The samples were equilibrated for 10 min at room temperature to allow the intercalating complex to bind. The nonintercalating Ru(tpy)(bpy)-O^{2+} was then added to the solutions, and the cleavage reactions were carried out as described above.

Results

Oxidation Mechanism. The complex Ru(tpy)(bpy)O^{2+} cleaves DNA by guanine oxidation and by sugar oxidation at the 1′ position.[18] The guanine oxidation must occur via an inner-sphere mechanism, since the redox potential for one-electron oxidation by Ru(tpy)(bpy)O^{2+} is much lower than the redox potential of guanine.[21] The sugar oxidation occurs by a similar oxo-transfer-type mechanism that generates a furanone at the 1′ position. The cleavage selectivity is a function of electrostatic recognition,[22] chemical reactivity of the oxidized functionality,[23] and solvent accessibility of the oxidized function in the biopolymer.[15] The binding affinity of the complex can be assessed using the reduced form, Ru(tpy)(bpy)OH_2^{2+}, which does not cleave DNA and can therefore be studied using fluorescence titration,[24] absorbance titration,[25] and equilibrium dialysis. Analysis of the ionic strength dependence of the binding affinity using polyelectrolyte theory shows that there is no detectable affinity other than that arising from the electrostatic interaction of the dicationic complex with the DNA polyanion.[22]

Direct participation of the oxo ligand of complexes based on Ru(tpy)(bpy)O^{2+} in the oxidation of small molecules is provided by numerous lines of evidence, including isotopic labeling and the observation of inner-sphere alkoxide intermediates.[26] Thus, it is likely that the DNA sugar oxidation involves direct attack of the oxo ligand at the 1′ position. We have shown previously that oxidation of calf thymus DNA by Ru(tpy)(bpy)O^{2+} yields the furanone 5-MF that is expected from 1′ oxidation (Scheme 2).[18] To confirm direct participation of the oxo ligand, the oxidation of calf thymus DNA was performed with Ru(tpy)-(bpy)$^{16}O^{2+}$ in $H_2{}^{18}O$ (98%). The experiment is complicated by the facile exchange of the oxo ligand with the solvent, but nonetheless, the mass of the recovered 5-MF by GC-MS was 40% at 96 amu and 60% at 98 amu. *Thus, 40% of the recovered 5-MF contained an oxygen derived directly from the metal complex.* A similar experiment has been used by Meunier et al. to support an oxygen rebound mechanism for DNA oxidation by Mn porphyrins and persulfate.[27] In this case, "redox tautomerism" led to exchange of the oxo ligand prior to DNA oxidation and a 50/50 ratio of 96 and 98 amu 5-MF. Similarly, it is likely that the 5-MF at 98 amu in the Ru(tpy)(bpy)O^{2+} reaction arises from exchange of the oxo ligand prior to DNA oxidation and not an alternative mechanistic pathway.

Table 1. Relative Cleavage Intensities at Individual Sites for Single-Strand (ss) and Duplex (ds) Forms of d[5′-$A_1T_2A_3C_4G_5C_6A_7A_8G_9G_{10}G_{11}C_{12}A_{13}T_{14}$][a]

	C4	G5	C6	A7	A8	G9	G10	G11	C12	A13
					Ru(tpy)(bpy)O^{2+} [b]					
ss	20	90	20	6	4	50	100	70	10	10
ds	1	130	20	9	20	70	100	60	30	30
					Ru(tpy)(dppz)O^{2+}					
ss	120	140	100	20	10	30	100	100	20	20
ds	30	6	< 3	< 1	< 1	4	100	8	<1	<1

[a] Cleavage intensities were obtained by integration of the optical density as a function of the band area using an Apple OneScanner and the Image program from the NIH, as described in the Experimental Section. All intensities were recorded using 30 μM of the metal complex and are relative to G_{10} for each case. Errors are ±10%. [b] Data taken from ref 15.

The complex Ru(tpy)(dppz)O^{2+} has identical electronic properties to Ru(tpy)(bpy)O^{2+} and differs only by the addition of the intercalating dppz ligand.[14] The binding affinity for Ru-(tpy)(dppz)OH_2^{2+} is comprised of a contribution from classical intercalation (6 kcal/mol) and the same electrostatic contribution observed for Ru(tpy)(bpy)O^{2+} (2.7 kcal/mol at 75 mM Na^+).[24] Viscometry, topisomerase inhibition,[1] and scanning force microscopy experiments[28] show that Ru(tpy)(dppz)O^{2+} unwinds and lengthens DNA in the manner for classical intercalation, and the lengthening of DNA and the nonelectrostatic binding affinity are both similar to those of ethidium bromide. Despite the addition of the intercalating moiety, the oxidation of DNA by Ru(tpy)(dppz)O^{2+} appears to proceed via the same mechanism as for Ru(tpy)(bpy)O^{2+}. Calf thymus DNA was oxidized by Ru(tpy)(dppz)O^{2+}, and the organic products were extracted and analyzed by HPLC (chromatogram shown in Supporting Information). As with Ru(tpy)(bpy)O^{2+}, the formation of 5-MF was confirmed by comigration of an authentic sample and observation of the expected mass upon reanalysis by GC−MS. Because the location of the 1′ hydrogen in duplex DNA is deep within the minor groove,[29] this experiment provides strong evidence that sugar oxidation by Ru(tpy)(dppz)O^{2+} occurs from complexes bound in the minor groove.

The selectivity of DNA oxidation by Ru(tpy)(dppz)O^{2+} was assessed by oxidation of a random coil oligomer d[5′-$A_1T_2C_3G_4C_5A_6A_7G_8G_9G_{10}C_{11}A_{12}T_{13}$] in its single-stranded and duplex forms followed by analysis using high-resolution electrophoresis. We have reported related experiments along with the concentration dependence and kinetic model for oxidation of the same oligomer by Ru(tpy)(bpy)O^{2+}.[15] The results for both complexes are shown in Table 1, which gives the extent of cleavage at each site in the oligomer relative to G10, which is the most intense site for Ru(tpy)(bpy)O^{2+} in the single-

(21) Steenken, S.; Jovanovic, S. V. *J. Am. Chem. Soc.* **1997**, *119*, 617−618.
(22) Kalsbeck, W. A.; Thorp, H. H. *Inorg. Chem.* **1994**, *33*, 3427−3429.
(23) Neyhart, G. A.; Cheng, C.-C.; Thorp, H. H. *J. Am. Chem. Soc.* **1995**, *117*, 1463−1471.
(24) Kalsbeck, W. A.; Thorp, H. H. *J. Am. Chem. Soc.* **1993**, *115*, 7146−7151.
(25) Smith, S. R.; Neyhart, G. A.; Kalsbeck, W. A.; Thorp, H. H. *New J. Chem.* **1994**, *18*, 397−406.
(26) Stultz, L. K.; Binstead, R. A.; Reynolds, M. S.; Meyer, T. J. *J. Am. Chem. Soc.* **1995**, *117*, 2520−2532.
(27) Pitié, M.; Bernadou, J.; Meunier, B. *J. Am. Chem. Soc.* **1995**, *117*, 2935−2936.
(28) Coury, J. E.; Anderson, J. R.; McFail-Isom, L.; Williams, L. D.; Bottomley, L. A. *J. Am. Chem. Soc.* **1997**, *119*, 3792−3796.
(29) Pratviel, G.; Bernadou, J.; Meunier, B. *Agnew. Chem., Int. Ed. Engl.* **1995**, *38*, 746−769.

stranded form. Briefly summarizing the published Ru(tpy)(bpy)O^{2+} results, the guanine oxidation is more efficient than the sugar oxidation in single-stranded DNA by about a factor of 7; this same ratio is obtained either from cleavage intensities on sequencing gels or from rate constants measured by optical spectroscopy for oxidation of mononucleotides. The guanine/sugar ratio is reduced upon hybridization to the duplex form, apparently because of a greater steric demand in the guanine oxidation compared to the sugar oxidation. This conclusion was supported by experiments using bulkier derivatives of Ru(tpy)(bpy)O^{2+}, which exhibited lower guanine/sugar ratios.[15]

For Ru(tpy)(dppz)O^{2+}, the intrinsic guanine/sugar ratio in the single-stranded form is significantly lower than for Ru(tpy)(bpy)O^{2+}; the cleavage intensities give a ratio of 2 for Ru(tpy)(dppz)O^{2+} compared to 7 for Ru(tpy)(bpy)O^{2+}. Although we have not measured the rate constants for mononucleotides with Ru(tpy)(dppz)O^{2+}, experiments on Ru(tpy)(bpy)O^{2+} show that both single-stranded cleavage intensities and rate constants give the same ratio, as stated above. Upon hybridization to the duplex form, however, a large change in specificity is observed with Ru(tpy)(dppz)O^{2+} that is strikingly evident in Table 1. The most intense site in the duplex form is G10, which was not the most intense site in the single-stranded form. In fact, cleavage of G10 is an order of magnitude more intense than every site in the oligonucleotide except for C4. By contrast, the cleavage of the duplex by Ru(tpy)(bpy)O^{2+} is actually *less* specific than cleavage of the single strand; for example, cleavage of A7, A8, C12, and A13 by Ru(tpy)(bpy)O^{2+} actually increases relative to G10 upon hybridization because of the steric effect on guanine oxidation. Thus, cleavage of single-stranded and duplex DNA by Ru(tpy)(bpy)O^{2+} are both relatively nonspecific (as is cleavage of single-stranded DNA by Ru(tpy)(dppz)O^{2+}), but cleavage of duplex DNA by Ru(tpy)(dppz)O^{2+} shows significantly increased reaction at a single site. Given the similarity in electronic properties and chemical mechanism of DNA oxidation, this difference must result from the recognition properties of the intercalative dppz ligand.

tRNA. We chose tRNA as a second target on which to evaluate the differences between Ru(tpy)(dppz)O^{2+} and Ru(tpy)(bpy)O^{2+} because the X-ray crystal structure of $tRNA^{Phe}$ is available,[30,31] and the tRNA conformation can be controlled in a relatively well-defined way by changing the salt concentration.[32] Therefore, cleavage patterns should be different for the native form and the semidenatured form where only the cloverleaf secondary structure is present.[19] For any thermal cleavage agent, oxidation of a given site could result from special recognition, chemical reactivity, or accessibility of that site. The latter sites, such as single-stranded guanines, will be targeted by both complexes. If only the cleavage pattern for Ru(tpy)(dppz)O^{2+} were available, distinguishing the sites that resulted from intercalative recognition would be problematic; however, the *comparison* of the cleavage patterns for Ru(tpy)(bpy)O^{2+} and Ru(tpy)(dppz)O^{2+} will better indicate sites that are targeted because of intercalative recognition, as seen with the single-stranded and duplex oligonucleotides. As we have discussed in detail elsewhere, the 2′-hydroxyl of ribose deactivates RNA sugars toward oxidation compared to DNA.[23] Therefore, only particularly oxidizable sugars in RNA are reactive toward Ru(tpy)(bpy)O^{2+}, leading to cleavage patterns that show primarily guanine oxidation.

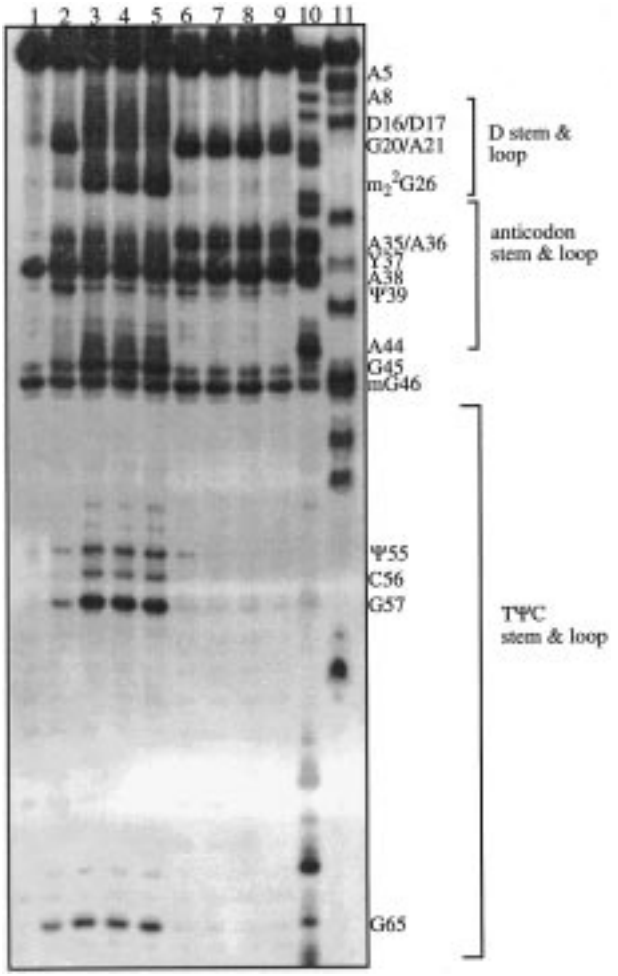

Figure 1. Gel showing the effect Pt(tpy)$(HET)^+$ has on the cleavage of 3′-^{32}P-$tRNA^{Phe}$ by Ru(tpy)(bpy)O^{2+}. Reactions in lanes 2−5 were done in the absence of $MgCl_2$ (semidenatured tRNA), while those in lanes 6−9 were done in the presence of 10 mM $MgCl_2$ (folded tRNA). All reactions were aniline-treated, and the final concentration of [Ru(IV)O^{2+}]was 200 μM. Lane 1 is the RNA control; lanes 2 and 6, RNA + [Ru(IV)O^{2+}]; lanes 3 and 7, 50 μM Pt(tpy)$(HET)^+$ + [Ru(IV)O^{2+}]; lanes 4 and 8, 75 μM Pt(tpy)$(HET)^+$ + [Ru(IV)O^{2+}]; lanes 5 and 9; 100 μM Pt(tpy)$(HET)^+$ + [Ru(IV)O^{2+}]; lane 10, A-lane (DEPC); and lane 11, U-lane (hydrazine).

Oxidation of folded $tRNA^{Phe}$ (10 mM sodium phosphate, pH 7.1, 10 mM $MgCl_2$) by Ru(tpy)(bpy)O^{2+} produced aniline-labile scission as visualized by polyacrylamide gel electrophoresis performed on the 3′ labeled tRNA (Figure 1). For the folded tRNA, cleavage was observed largely at guanine and adenine sites in the D and anticodon loops plus a very weak site at Ψ55 in the TΨC loop (Figure 2), which is close to the D loop in the tertiary structure. Oxidation of the semidenatured form of $tRNA^{Phe}$ (10 mM sodium phosphate, pH 7.1, no $MgCl_2$) produced cleavage at a few additional sites at stem−loop junctions, the variable loop, and the TΨC loop that, according to the X-ray crystal structure, are expected to be protected from oxidation in the folded form.[33] Our results are consistent with an earlier chemical modification study which showed that the accessibility of A, C, G, and T sites within the TΨC loop increases upon denaturation of tRNA.[34]

Cleavage of folded $tRNA^{Phe}$ (10 mM sodium phosphate, pH 7.1, 10 mM $MgCl_2$) by Ru(tpy)(dppz)O^{2+} produces no cleavages

(30) Jack, A.; Ladner, J. E.; Klug, A. *J. Mol. Biol.* **1976**, *108*, 619−649.
(31) Jack, A.; Ladner, J. E.; Rhodes, D.; Brown, R. S.; Klug, A. *J. Mol. Biol.* **1977**, *111*, 315−328.
(32) Chen, X.; Woodson, S. A.; Burrows, C. J.; Rokita, S. E. *Biochemistry* **1993**, *32*, 7610−7616.
(33) Lavery, R.; Pullman, A. *Biophys. Chem.* **1984**, *19*, 171−184.
(34) Peattie, D.; Gilbert, W. *Proc. Natl. Acad. Sci. U.S.A.* **1980**, *77*, 4679−4682.

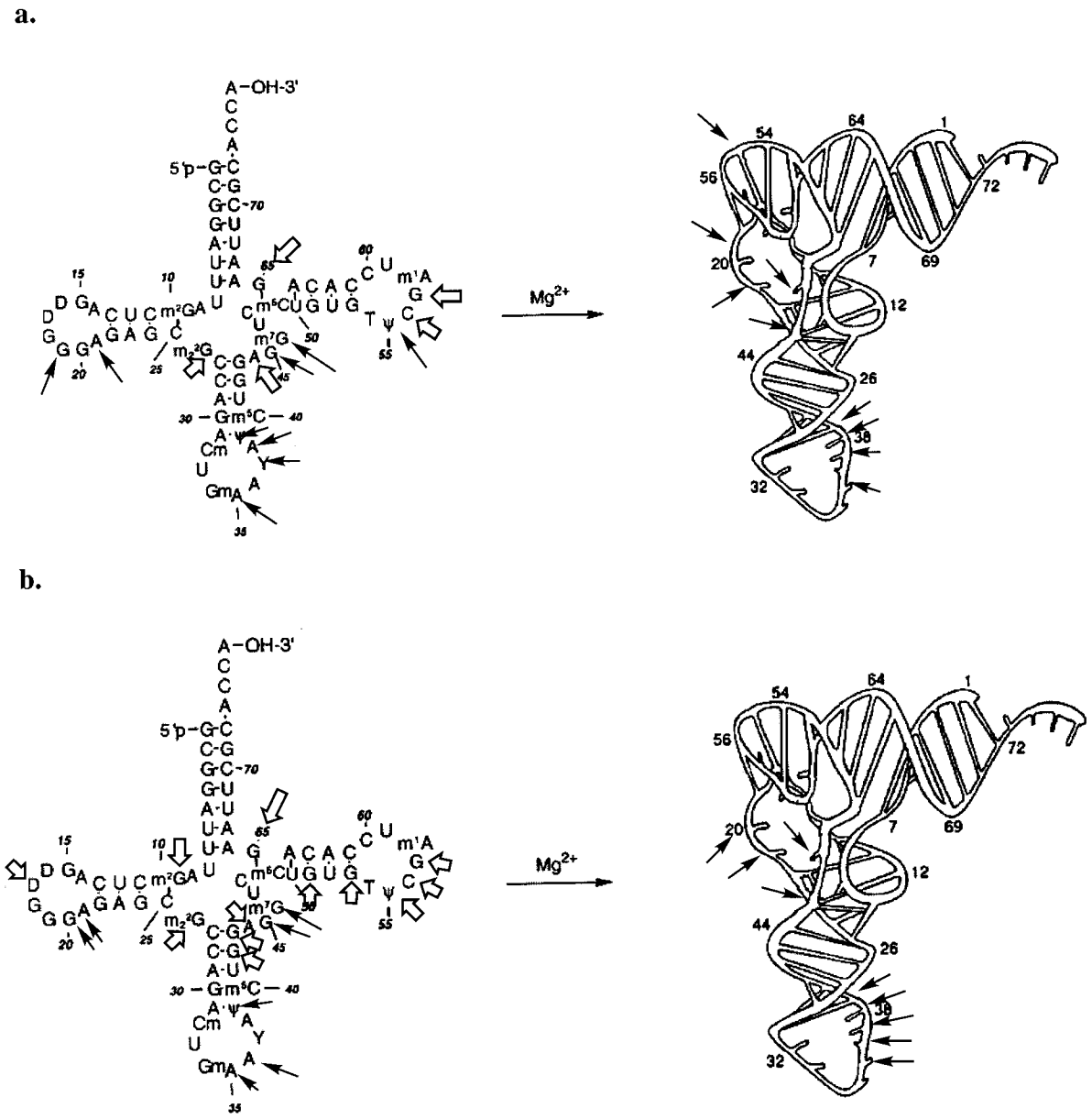

Figure 2. Sites of aniline-labile cleavage for 3′-^{32}P-labeled tRNA^{Phe} following oxidation by (a) Ru(tpy)(bpy)O^{2+} and (b) Ru(tpy)(dppz)O^{2+}. Solid arrows represent cleavage sites for both the folded (10 mM $MgCl_2$) and semidenatured (no added Mg^{2+}) forms. Open arrows indicate sites observed only in the semidenatured form.

in double-stranded regions (Figure 2) with the exception of Ψ39, which is adjacent the anticodon loop and therefore is solvent accessible. In fact, the cleavage pattern for the folded tRNA is very similar to that for Ru(tpy)(bpy)O^{2+} with cleavage only in the D and anticodon loops. However, cleavage of the semidenatured tRNA^{Phe} by Ru(tpy)(dppz)O^{2+} produces a larger number of cleavages than Ru(tpy)(bpy)O^{2+}, including five new double-stranded sites. This result implies that the helixes in the unfolded secondary structure can accommodate the octahedral metallointercalator. This intercalation into the TΨC and anticodon helixes is apparently precluded by the folded structure, so the cleavage patterns for Ru(tpy)(bpy)O^{2+} and Ru(tpy)(dppz)-O^{2+} are the same for folded tRNA. The cleavage patterns for Ru(tpy)(dppz)O^{2+} and Ru(tpy)(bpy)O^{2+} with tRNA are summarized in Table 2.

The results in Figure 1 suggest strongly that Ru(tpy)(dppz)-O^{2+} intercalates into semidenatured tRNA but not into folded tRNA; however, in studying these reactions, we want to preclude the possibility that the binding of the biomolecule by the unreacted Ru(tpy)(dppz)O^{2+} metallointercalator alters the structure in some way and then renders the biomolecule more reactive toward a second equivalent of the oxidant. We therefore have chosen to study reactions of the nonintercalating Ru(tpy)(bpy)-O^{2+} complex in the presence of an exogenous intercalator that does not cleave DNA. The complex Pt(tpy)$(HET)^+$ has been shown to lengthen calf thymus DNA and unwind DNA in a manner that is consistent with intercalation,[12] and a crystal structure of Pt(tpy)$(HET)^+$ bound to the deoxyCpG dimer demonstrates that the planar, aromatic terpyridine ligand of this complex inserts between the 2 GC base pairs.[11] The Pt intercalator, unlike many organic intercalators, is redox inert and does not reduce Ru(tpy)(bpy)O^{2+}. We therefore investigated the cleavage pattern of Ru(tpy)(bpy)O^{2+} with and without Pt(tpy)$(HET)^+$ to determine the effect of decoupling the intercalative recognition and oxidation chemistry.

When the intercalating Pt(tpy)$(HET)^+$ is added to folded tRNA, no change in the cleavage pattern or intensities for Ru-(tpy)(bpy)O^{2+} was observed (Figure 1), further indicating that

Table 2. Relative Cleavage Intensities[a] at Individual Sites for Semidenatured and Folded $TRNA^{Phe}$

	$Ru(tpy)(bpy)O^{2+}$				$Ru(tpy)(dppz)O^{2+}$	
	semidenatured	semidenatured + Pt(tpy) $(HET)^+$	folded	folded + Pt(tpy) $(HET)^+$	semidenatured	folded
m^2G10		v. weak			v. weak	
D17		v. weak			v. weak	
G19	med	v. weak	strong	strong		
G20					v. weak	strong
A21	strong		strong	strong	v. weak	strong
m_2^2G26	weak	strong			medium	
Gm34			strong	strong		
A35	strong	med	strong	strong	med	med
A36		weak			med	med
Y37	med	weak	med	med		weak
A38	med	weak	med	med		weak
Ψ39	strong	med	weak	weak	strong	strong
G42		weak			strong	
G43		med			strong	
A44	v. weak	med			weak	
G45	v. weak	strong	v. weak	v. weak	v. weak	v. weak
m^7G46	v. weak	weak	v. weak	v. weak	v. weak	v. weak
G51		v. weak			weak	
G53		v. weak			weak	
Ψ54		v. weak			v. weak	
Ψ55	weak	med	v. weak	v. weak	strong	
C56	v. weak	med			weak	
G57	med	strong			strong	
G65	med	strong			strong	

[a] Relative cleavage intensities were assessed by visual inspection of the autoradiograms and are recorded on a scale of very weak to strong (strong indicates the most intense bands), and the intensities for the sites within a single lane are relative to each other. The concentration for each of the oxoruthenium complexes was 200 μM, and the concentration of $Pt(tpy)(HET)^+$ was 100 μM.

the folded structure does not permit intercalative binding. On the other hand, addition of $Pt(tpy)(HET)^+$ to a $Ru(tpy)(bpy)O^{2+}$ cleavage reaction of semidenatured tRNA (no Mg^{2+}) changed the cleavage pattern and increased the intensities of several bands, particularly in the D and TΨC stem and loop regions (Figure 1). Lanes 3−5 appear identical because the dissociation constant of $Pt(tpy)(HET)^+$ is < 50 μM. Cleavage enhancements are observed at m_2^2G26, G65, Ψ55, G56, and m^2G10, which are all involved in tertiary interactions in the folded form.[35] This result strongly suggests that binding of the exogenous intercalator changes the structure of the semidenatured tRNA and renders more sites accessible to the $Ru(tpy)(bpy)O^{2+}$ oxidant. This is consistent with an earlier discovery that ethidium bromide destabilizes tRNA structure in the absence of magnesium ion.[36] The collective results, summarized in Table 2, point to an inability of folded tRNA to accommodate intercalators while the semidenatured form can bind both the $Ru(tpy)(dppz)O^{2+}$ and $Pt(tpy)(HET)^+$ intercalators. Furthermore, the findings suggest that the additional cleavage sites observed for $Ru(tpy)(dppz)O^{2+}$ but not for $Ru(tpy)(bpy)O^{2+}$ in the semidenatured form result from a combination of both intercalative recognition and a structural perturbation resulting from this intercalative binding.

Bulge−Loop Structures. Bulge−loop structures found in noncoding regions of mRNA regulate the expression of both ferritin[37−39] and the HIV-1 viral genome,[40−43] and related structures are found frequently during in vitro selection of protein-binding aptamers via the SELEX process.[44] Intercalators target the bulge and bulge−stem junctions of these structures and serve as promising candidates for drugs that inhibit binding of proteins to bulge−loop sequences.[45−49] We therefore have examined the oxidation of both DNA and RNA bulge−loop structures with $Ru(tpy)(bpy)O^{2+}$ and $Ru(tpy)(dppz)O^{2+}$. The sequences we have chosen are the TAR RNA sequence from HIV-1 and its DNA analogue (Figure 3). We chose to study both the RNA and its DNA analogue because of the difficulty in visualizing the sugar reaction in RNA; the DNA analogue has been studied previously with enediynes for similar reasons.[46] Also, there has been considerable interest in studying the similarities between folded tRNA and tDNA[50−52] and we wondered whether similarities existed between bulge−loop structures.

As expected, the loop guanines in TAR DNA (Figure 4) and TAR RNA (Figure 5) are oxidized more efficiently than the stem guanines, although the double-stranded G11 adjacent to the bulge is quite reactive in the TAR DNA. This enhanced reactivity is almost certainly the result of an increase in solvent accessibility at this site due to the presence of the bulge. In contrast, a high reactivity was not seen at G11 for the TAR

(35) Sussman, J. L.; Kim, S.-H. *Science* **1976**, *192*, 853−858.
(36) Urbanke, C.; Römer, R.; Maass, G. *Eur. J. Biochem.* **1973**, *33*, 511−516.
(37) Theil, E. C. *Biofactors* **1993**, *4*, 87−93.
(38) Theil, E. C. *J. Biol. Chem.* **1990**, *265*, 4771−4774.
(39) O'Halloran, T. V. *Science* **1993**, *261*, 715−725.
(40) Dingwall, C.; Ernberg, I.; Gait, M. J.; Green, S. H.; Heaphy, S.; Karn, J.; Lowe, A. D.; Singh, M.; Skinner, M. A. *EMBO J.* **1990**, *9*, 4145−4153.
(41) Kao, S.-Y.; Calman, A. F.; Luciw, P. A.; Peterlin, B. M. *Nature* **1987**, *330*, 489−493.
(42) Marciniak, R. A.; Calnan, B. J.; Frankel, A. D.; Sharp, P. A. *Cell* **1990**, *63*, 791−802.
(43) Selby, M. J.; Bain, E. S.; Luciw, P. A.; Peterlin, B. M. *Genes Dev.* **1989**, *3*, 547−558.
(44) Gold, L.; Polisky, B.; Uhlenbeck, O.; Yarus, M. *Annu. Rev. Biochem.* **1995**, *64*, 763−97.
(45) Kean, J. M.; White, S. A.; Draper, D. E. *Biochemistry* **1985**, *24*, 5062−5070.
(46) Kappen, L. S.; Goldberg, I. H. *Biochemistry* **1994**, *34*, 5997−6002.
(47) Neenhold, H. R.; Rana, T. M. *Biochemistry* **1995**, *34*, 6303−6309.
(48) Ratmeyer, L. S.; Vinayak, R.; Zon, G.; Wilson, W. D. *J. Med. Chem.* **1992**, *35*, 966−968.
(49) Wilson, W. D.; Ratmeyer, L.; Cegla, M. T.; Spychala, J.; Boykin, D.; Demeunynck, M.; Lhomme, J.; Krishnan, G.; Kennedy, D.; Vinayak, R.; Zon, G. *New J. Chem.* **1994**, *18*, 419−423.
(50) Hecht, S. M. *Bioconjugate Chem.* **1994**, *5*, 513−526.
(51) Lim, A. C.; Barton, J. K. *Biochemistry* **1993**, *32*, 11029−11034.
(52) Holmes, C. E.; Abraham, A. T.; Hecht, S. M.; Florentz, C.; Giege, R. *Nucleic Acids Res.* **1996**, *24*, 3399−3406.

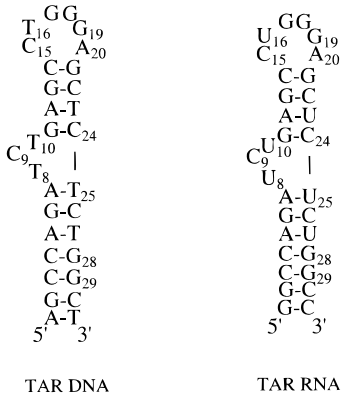

Figure 3. Sequence and secondary structures of TAR RNA and TAR DNA analogue.

Table 3. Relative Cleavage Intensities at Individual Sites for TAR DNA and TAR RNA[a]

	TAR DNA		TAR RNA	
	Ru(tpy)(bpy)O^{2+}	Ru(tpy)(dppz)O^{2+}	Ru(tpy)(bpy)O^{2+}	Ru(tpy)(dppz)O^{2+}
G6	50	30	8	9
A7	1	<1	–	–
T/U8	<1[b]	30	–	–
C9	30[b]	200	–	–
T/U10	20[b]	80	-	–
G11	150[b]	150	60[b]	70
G13	2	4	10	20
T/U16	<1	6	–[c]	–
G17	100	100	100[c]	100
G18	40	50	70[c]	100
G19	3	10	30[c]	70
G21	4	<1	20[b]	30
T25	4[b]	–	–	–
C26	<1[b]	–	–	–
G28	<1	<1	n.a.	n.a.

[a] All intensities were recorded using 100 μM of the oxoruthenium complex and are relative to G_{17} in each case. The dashed lines indicate that no cleavage was detected at those sites, and n.a. indicates that cleavage information was not available for that site. Errors are ±10%. [b] Sites that were inhibited the most upon addition of Pt(tpy)$(HET)^+$. [c] Sites that exhibited an increase in intensity upon addition of Pt(tpy)$(HET)^+$.

RNA, which is probably due to differences between the RNA and DNA structures. Both the DNA and RNA samples were annealed, and the hairpin formation was confirmed by analysis on a native gel, so a differential ability to form the hairpin structure is not the origin of this difference. Rather, the greater ability of RNA to fold into tighter structures stabilized by the hydrogen bonding of the 2′-hydroxyl[53] probably is the source of differences between the structures, and hence it is not surprising that the solvent accessibility of G11 is different for the DNA.

The extent of sugar oxidation for Ru(tpy)(bpy)O^{2+} is slightly larger at the loop and bulge sites in TAR DNA (Figure 4) where the 1′ hydrogens are more accessible compared to sites within the double-stranded stem regions. Sugar oxidation within the stem is relatively sequence-independent for all the sites with the exception that T25 shows slightly enhanced cleavage; the high reactivity of T25 is probably due to its proximity to the bulge on the opposite strand. The same loop and stem sites are observed for Ru(tpy)(dppz)O^{2+}, except that the intercalating complex shows significantly enhanced cleavage at T10 and C9 within the bulge. Surprisingly, *the sugar oxidation at C9 is even stronger than oxidation at any of the guanine sites*, indicating a startling preference of Ru(tpy)(dppz)O^{2+} for the bulge region. This enhanced cleavage at C9 was also observed for 3′-labeled TAR DNA and is therefore not simply the result of overreaction. It has previously been shown that an intercalating cleavage reagent specifically cleaves at or near this trinucleotide bulge within a TAR DNA analogue,[46] and this result provides another example of this intercalative recognition.

Addition of Pt(tpy)$(HET)^+$ to the TAR DNA hairpin inhibited cleavage by Ru(tpy)(bpy)O^{2+} primarily opposite the bulge at T25 and C26 and also at C9 and T10 within the bulge (gel given in Supporting Information). These results further imply preferential binding of Pt(tpy)$(HET)^+$ to the bulge site, as observed for other intercalators, and support the idea that the strong preference for cleavage of C9 and T10 by Ru(tpy)(dppz)-O^{2+} is the result of intercalative recognition. Much weaker inhibition by Pt(tpy)$(HET)^+$ was observed within the double-helical stem of TAR DNA, as also expected for an intercalative binding mode. We observe only cleavage inhibition and no cleavage enhancement as a result of adding Pt(tpy)$(HET)^+$, suggesting that the exogenous intercalator does not grossly change the structure of the DNA and render new sites particularly reactive.

As stated above, almost exclusively guanine oxidation is observed for TAR RNA for both Ru(tpy)(dppz)O^{2+} and Ru-(tpy)(bpy)O^{2+}, which exhibited nearly identical cleavage patterns (Figure 5). The intercalating complex does show slightly more cleavage at G19 in the loop and G21 adjacent the loop, implying that intercalative recognition occurs at the loop. The hairpin loop has a very flexible structure in solution, but some studies have suggested partial ordering of the bases,[54] and although no direct evidence has been found for a G19−C15 Watson−Crick base pair, the presence of this base pair across the loop is consistent with NMR results[55] and could provide a site for intercalation. Accordingly, efficient cleavage by $Rh(phen)_2phi^{3+}$ (phi = 9,10-phenanthrenequinone diimine, phen = 1,10-phenanthroline) was also found at bases within the loop,[47] further indicating that this is a possible site for intercalative recognition. The comparison of the cleavage patterns for Ru(tpy)(dppz)O^{2+} and Ru(tpy)(bpy)O^{2+} supports this possibility.

As was observed for the TAR DNA analogue, cleavage of the RNA by Ru(tpy)(bpy)O^{2+} is inhibited at several sites upon binding of Pt(tpy)$(HET)^+$ (gel shown in Supporting Information). Again, due to the decreased reactivity of the sugar sites, we were unable to assess any cleavage inhibition at the sugar sites. The largest degree of cleavage inhibition was observed at G11 adjacent the bulge, again supporting intercalation at or directly adjacent to the bulge. A smaller amount of inhibition was observed at G21 adjacent the loop, again supporting a modest preference for intercalative recognition in the loop. The results of TAR oxidation are summarized in Table 3.

Unlike with the DNA analogue, several sites within the RNA loop were observed where cleavage by Ru(tpy)(bpy)O^{2+} was enhanced upon addition of Pt(tpy)$(HET)^+$. Several guanine sites within the loop exhibited increased reactivity, and U16 in the loop surprisingly became reactive despite being a sugar site. This increase in reactivity within the loop suggests that binding of the intercalator to the bulge or to some other site changes the structure of the loop to make it more reactive toward the oxidant. This structural change is not observed for the TAR DNA analogue, which suggests that the ability to sense structural changes at a remote site is much greater for RNA than for DNA,

(53) Celander, D. W.; Cech, T. R. *Science* **1991**, *251*, 401.
(54) Loret, E.; Georgel, P.; Johnson, W. C.; Ho, P. S. *Proc. Natl. Acad. Sci. U.S.A.* **1992**, *89*, 9734−9738.
(55) Jaeger, J. A.; Tinoco, I., Jr. *Biochemistry* **1993**, *32*, 12522−12530.

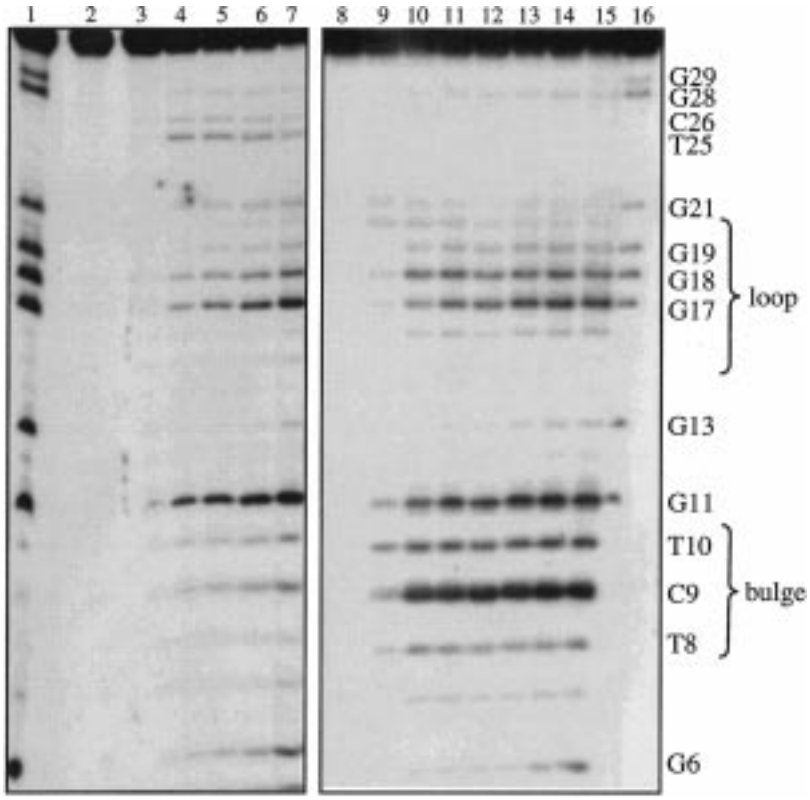

Figure 4. Cleavage of TAR DNA by Ru(tpy)(bpy)O^{2+} and Ru(tpy)(dppz)O^{2+}. The DNA concentrations are provided in the experimental section, and all samples were treated with piperidine (90 °C; 30 min). Lanes 1 and 16 are Maxam−Gilbert G lanes; lanes 2−7, DNA + 0, 10, 30, 50, 70, and 100 μM Ru(tpy)(bpy)O^{2+}, respectively; lanes 8−15, DNA + 0, 20, 40, 60, 70, 80, 90, and 100 μM Ru(tpy)(dppz)O^{2+}, respectively.

which is consistent with a more tightly folded structure for RNA. A similar increase did not occur at G11 (in fact, cleavage of G11 was inhibited by Pt(tpy)$(HET)^{+}$), which is near the bulge site and suggests that no structural change occurred at the bulge. This finding parallels many studies in RNA; for example, binding of the regulatory protein to the stem−loop iron recognition element mRNA is exquisitely sensitive to the bases in the flanking region many base pairs from the protein binding site.[56]

Discussion

Chemical Mechanism. The isotopic labeling experiment shows that the collision leading to sugar oxidation must be one in which Ru(tpy)(bpy)O^{2+} is close enough to the 1′ hydrogen to transfer the oxygen atom from the metal complex directly to the deoxyribose. This result is in agreement with our earlier report that distamycin inhibits the sugar reaction in a predictable manner for an oligonucleotide that has been structurally characterized with bound distamycin.[18] In this case, the distamycin protects the sugars in the minor groove that are known to be in contact with the drug in the X-ray crystal structure.[57,58] This result is consistent with the isotopic labeling experiment, because only from the minor groove side can Ru(tpy)(bpy)O^{2+} approach the 1′ hydrogen closely enough to transfer the oxygen atom. Likewise, the guanine oxidation has been shown previously to occur via an intermediate that has been detected spectroscopically and is likely an inner-sphere complex of Ru(tpy)(bpy)O^{2+} and guanine, possibly a Ru^{III}−O−G intermediate.[23] Thus, experiments on the chemical mechanism show that the complex must be in intimate contact with both the guanine and sugar during the oxidation process, as has also been shown for Mn porphyrin/persulfate reactions,[27] the enediynes,[59,60] and Ni complexes where precoordination to guanine is a requirement for cleavage.[61−63] These reactions are in contrast to those that damage DNA by generating a diffusible intermediate, such as •OH,[64] or those that oxidize guanine by outer-sphere electron transfer, which can occur over larger distances via tunneling.[7,65] Therefore, cleavage sites of Ru(tpy)(bpy)O^{2+} and related complexes reflect the preference of the complex to bind at the oxidized site.

The findings that the chemical mechanism of Ru(tpy)(dppz)O^{2+} is the same as for Ru(tpy)(bpy)O^{2+} now shows that the cleavage sites of the intercalating complex also reflect the binding preferences. The studies reported here are therefore the first in which the binding preferences of a dppz complex can be determined by high-resolution gel electrophoresis. The only other studies involving DNA cleavage by a dppz complex are those in which the complex damages guanine by long-range electron transfer, which does not depend on the binding

(56) Dix, D. J.; Lin, P.-N.; McKenzie, A. R.; Walden, W. E.; Theil, E. C. *J. Mol. Biol.* **1993**, *231*, 230−240.
(57) Kennard, O.; Hunter, W. N. *Angew. Chem., Int. Ed. Engl.* **1991**, *30*, 1254−1277.
(58) Coll, M.; Frederick, C. A.; Wang, A. H.-J.; Rich, A. *Proc. Natl. Acad. Sci. U.S.A.* **1987**, *84*, 8385−8389.
(59) Frank, B. L.; Worth, L.; Christner, D. F.; Kozarich, J. W.; Stubbe, J.; Kappen, L. S.; Goldberg, I. H. *J. Am. Chem. Soc.* **1991**, *113*, 2271−2275.
(60) Myers, A. G.; Cohen, S. B.; Kwon, B. M. *J. Am. Chem. Soc.* **1994**, *116*, 1670−1682.
(61) Muller, J. G.; Zheng, P.; Rokita, S. E.; Burrows, C. J. *J. Am. Chem. Soc.* **1996**, *118*, 2320−2325.
(62) Chen, X.; Woodson, S. A.; Burrows, C. J.; Rokita, S. E. *Biochemistry* **1993**, *32*, 7610−7616.
(63) Burrows, C. J.; Rokita, S. E. *Acc. Chem. Res* **1994**, *27*, 295−301.
(64) Dixon, W. J.; Hayes, J. J.; Levin, J. R.; Weidner, M. F.; Dombroski, B. A.; Tullius, T. D. *Methods Enzymol.* **1991**, *208*, 380−413.
(65) Arkin, M. R.; Stemp, E. D. A.; Pulver, S. C.; Barton, J. K. *Chem. Biol.* **1997**, *4*, 389−400.

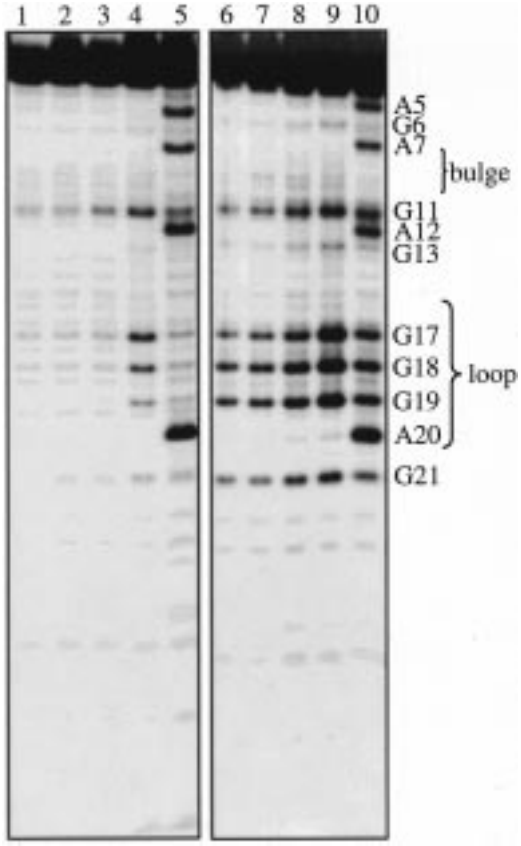

Figure 5. Cleavage of TAR RNA by Ru(tpy)(bpy)O^{2+} and Ru(tpy)(dppz)O^{2+}. The RNA concentrations are provided in the experimental section, and all samples were treated with aniline, as described. Lanes 2−4 were done with varying concentrations of Ru(tpy)(bpy)O^{2+}, while lanes 7−9 were done with varying concentrations of Ru(tpy)(dppz)O^{2+}. Lanes 1−4 are RNA + 0, 20, 50, and 100 μM Ru(tpy)(bpy)O^{2+}; lanes 6−9, RNA + 0, 20, 50, and 100 μM Ru(tpy)(dppz)O^{2+}; Lanes 5 and 10 are A-lanes (DEPC).

preference of the complex.[7] In fact, outer-sphere guanine oxidation occurs equally at all guanines of similar redox potential, showing that subtle differences in binding of the complex are not important in determining the relative intensities of the cleavage sites.[65] Thus, the results described here provide the first look at how the dppz intercalator influences the cleavage selectivity. In particular, the observation of 5-MF following oxidation of duplex DNA by Ru(tpy)(dppz)O^{2+} must arise from attack of the complex on the minor groove side of the duplex. Thus, at least the fraction of the complex that produces sugar lesions is bound in the minor groove.

The issue of major versus minor groove binding by dppz complexes has been a subject of some controversy with evidence from NMR studies implicating both major or minor groove binding in different studies.[8,66] Our experiments here support association in minor groove binding during the collision that leads to strand scission with two important caveats. The first is that the sugar pathway is only responsible for a small fraction of the total amount of metal complex in the cleavage reaction; in the Ru(tpy)(bpy)O^{2+} system, 10% of the oxidant is consumed by sugar oxidation.[18] Therefore, our result does not exclude the possibility that the fraction of the metal complex that does not undergo sugar reaction (which is the major fraction) is bound in the major groove. Further, our experiments were done on a dppz complex where the remainder of the ligand set is tpy and oxo, whereas the other experiments addressing this issue were performed for complexes with either two ancillary bpy ligands or two ancillary phenanthroline ligands.[2,8,66]

Recognition. The effect of duplex formation on the cleavage pattern of Ru(tpy)(dppz)O^{2+} is dramatic (Table 1). For Ru(tpy)(bpy)O^{2+} the cleavage pattern becomes more regular upon duplex formation, probably because the guanine oxidation becomes less efficient due to steric occlusion of the oxidized guanine site, as we have discussed elsewhere.[15] In contrast, the cleavage pattern for Ru(tpy)(dppz)O^{2+} becomes much more specific upon duplex formation with reaction almost exclusively at a single site. The preference of the complex for the particular site could result either from the energetics of stacking of the intercalator in the site or from the ability of the site to distort in order to accommodate the intercalator. Binding of the complex in the minor groove will require significant distortion of the DNA to accommodate the dppz ligand in the minor groove. In either case, a strong effect of duplex formation on the cleavage pattern is consistent with intercalative recognition by the complex.

A similar effect of intercalative recognition is apparent in the tRNA studies. The folded tRNA cannot accommodate an intercalator because the associated helical unwinding will destroy the tertiary contacts required to maintain the folded structure.[53] Studies of ethidium bromide fluorescence support this point and show that intercalation can occur only in the acceptor stem,[67] which is located away from the tertiary contacts. Likewise, the cleavage pattern of Ru(tpy)(bpy)O^{2+} and Ru(tpy)(dppz)O^{2+} are quite similar for folded tRNA (Table 2), suggesting that the dppz complex cannot intercalate into folded tRNA. In contrast, cleavage of the semidenatured form by Ru(tpy)(dppz)O^{2+} produces a number of new sites compared to Ru(tpy)(bpy)O^{2+}, suggesting that the helixes in the semidenatured form can accommodate the intercalator.

Photocleavage experiments have also been performed on folded tRNA's with octahedral rhodium(III) metallointercalators.[51,68−70] For $Rh(phen)_2(phi)^{3+}$, recognition of folded tRNA does not involve classical intercalation into double-helical regions but rather shape-selective stacking of the phi ligand against exposed bases in sites of tertiary interactions, and as in our experiment, Mg^{2+} does not inhibit cleavage.[70] Incorporation of the intercalating function apparently does not lead to cleavage controlled by such a binding mode for Ru(tpy)(dppz)O^{2+}, because the cleavage pattern for the folded structure is the same as for the nonintercalating Ru(tpy)(bpy)O^{2+}. Because of the uncoordinated ring nitrogens, dppz is much less hydrophobic than phi, which may explain why the higher-order sites cleaved by rhodium intercalators are not recognized by Ru(tpy)(dppz)O^{2+}. The difference between the recognition pattern for Ru(tpy)(dppz)O^{2+} and those for the phi complexes emphasizes the importance of the steric effects and hydrophobicities of both the intercalator and the ancillary ligands;[71] comparison of the cleavage patterns for Ru(tpy)(bpy)O^{2+} and Ru(tpy)(dppz)O^{2+} on the semidenatured form strongly implicates intercalative

(66) Greguric, I.; Aldrich-Wright, J. R.; Collins, J. G. *J. Am. Chem. Soc.* **1997**, *199*, 33621−3622.

(67) Jones, C. R.; Boton, P. H.; Kearns, D. R. *Biochemistry* **1978**, *17*, 601−607.

(68) Chow, C. S.; Hartman, K. M.; Rawlings, S. L.; Huber, P. W.; Barton, J. K. *Biochemistry* **1992**, *31*, 3534−3542.

(69) Chow, C. S.; Barton, J. K. *Biochemistry* **1992**, *31*, 5423−5429.

(70) Chow, C. S.; Behlen, L. S.; Uhlenbeck, O. C.; Barton, J. K. *Biochemistry* **1992**, *31*, 972−982.

(71) Campisi, D.; Morii, T.; Rokita, S. E. *Biochemistry* **1994**, *33*, 4130−4139.

binding of dppz into RNA helixes, which is not realized with the phi complexes.[72]

Numerous studies have addressed binding of the classical intercalator ethidium bromide to tRNA.[36,67,73−75] These studies show that ethidium binds intercalatively to the native structure at a single site in folded $tRNA^{Phe}$ and at multiple (4−6) sites in the semidenatured form.[67,73] An X-ray crystal structure shows that when ethidium is added to tRNA crystals, binding occurs nonintercalatively to the outside of tRNA;[74] however, NMR and energy transfer studies show that binding in solution occurs by intercalation in the acceptor stem,[75,76] which would not distort the helixes that must fold to form the Mg^{2+} binding sites.[67] The difference in the number of intercalation sites for the two forms of tRNA is fully consistent with the results reported here for Ru(tpy)(dppz)O^{2+} with the exception that we did not observe any intercalation in the acceptor stem region of the folded tRNA where the single intercalation site was observed for the folded tRNA. This difference arises because the reactivity for base-paired residues other than gunaines is very low, and the implicated intercalation site is an AU site.[76]

Although the NMR studies implicate binding in only the acceptor stem, cleavage of folded $tRNA^{Phe}$ by the intercalator methidiumpropyl EDTA iron(II) (MPE·Fe^{II}) has been observed in both the acceptor stem and the anticodon helix.[45] In this study, 0.2 M Na^+ was used to stabilize the tertiary tRNA structure instead of Mg^{2+}, which may change the sensitivity of the folded structure to intercalation since assembly of specific Mg^{2+} binding sites is not required. In fact, fluorescence studies show that ethidium covalently attached to the D and anticodon stems is very solvent accessible in the presence of 1 mM Mg^{2+} but that ethidium is protected from solvent in the absence of Mg^{2+}, implying that intercalation is only precluded in the presence of Mg^{2+}.[77] These results have been used to suggest that at least 1 mM Mg^{2+} is required to stabilize the crystallographically characterized tRNA structure in solution. In a similar study,[78] relatively nonspecific cleavage by MPE·Fe(II) was observed, and the cleavage pattern was insensitive to temperature (20−37 °C) and Mg^{2+} concentration (0−10 mM). The higher Mg^{2+} concentrations did reduce cleavage but did not change the cleavage pattern, as we observed at higher Mg^{2+} concentration. The cleavage data were interpreted as consistent with binding of ethidium on the outside of the tRNA[74] and by intercalation in the acceptor stem.[67]

Binding of intercalators to bulge regions in hairpin loops has been observed for a variety of small molecules.[46−49] We therefore reasoned that if the dppz complex behaved similarly to classical intercalators, preferential binding to the bulge in the TAR sequences would occur. In fact, Ru(tpy)(dppz)O^{2+} oxidizes the bulge C9 in the TAR DNA sequence more efficiently than any other site (Table 3), despite the fact that sugar oxidation is chemically less efficient than guanine oxidation, while Ru(tpy)(bpy)O^{2+} does not have a strong preference for the bulge site. That the bulge in TAR DNA participates in intercalative recognition is also supported by the observation that Pt(tpy)$(HET)^+$ inhibits cleavage by Ru(tpy)(bpy)O^{2+} at C9 and the surrounding nucleotides. These results support previous analogies drawn similarly between cleavage of the bulge region in TAR RNA and TAR DNA by enediynes.[46]

In RNA, sugar oxidation is not observed to any significant extent; therefore, recognition of the bulge region in TAR RNA by Ru(tpy)(dppz)O^{2+} cannot be assessed in the same way as for the TAR DNA. Accordingly, the single-stranded guanines in the loop exhibit the highest reactivity toward both Ru(tpy)(dppz)O^{2+} and Ru(tpy)(bpy)O^{2+}. Nonetheless, the oxidation by Ru(tpy)(bpy)O^{2+} of the G11 site, which is close to the bulge region, is inhibited by the classical intercalator Pt(tpy)$(HET)^+$. In addition, the loop nucleotides become more reactive upon binding of Pt(tpy)$(HET)^+$, suggesting that binding of the intercalator to the bulge alters the loop conformation and renders the loop guanines more solvent accessible.

Model studies have illustrated that due to the presence of the trinucleotide bulge, the major groove of TAR RNA is not deep and narrow as in typical A form RNA but has about the same dimensions as B form DNA.[79,80] It is believed that this groove opening provides a binding pocket for the tat protein,[47,79,80] and likewise for intercalators that also recognize this distorted site.[46−49] The octahedral $Rh(phen)_2phi^{3+}$ does not bind double-helical or unstructured single-stranded RNA but is able to recognize the accessible groove within the helical stem of TAR RNA, resulting in cleavage primarily opposite the bulge.[47] NMR studies have shown that these bases opposite the bulge remain stacked, and therefore provide an optimal binding site for the phi ligand.[81] Incubation of neocarzinostatin with a TAR RNA analogue containing a triuracil bulge resulted in a single cleavage site at the U corresponding to C9 in the bulge, providing yet another example of intercalative recognition at bulge sites within RNA.[46] Our results presented above are consistent with both Ru(tpy)(dppz)O^{2+} and Pt(tpy)$(HET)^+$ intercalating at or adjacent the bulge in TAR RNA.

Conclusions

The studies described here provide the first look at the recognition properties of complexes of the dppz ligand as visualized by high-resolution electrophoresis. To elucidate the sites that specifically result from the presence of the intercalator, we have designed two comparisons of cleavage patterns. The first is the comparison of Ru(tpy)(dppz)O^{2+} and Ru(tpy)(bpy)O^{2+}, where the sites the two complexes have in common do not result from intercalation while the new sites for Ru(tpy)(dppz)O^{2+} clearly arise from recognition by the dppz ligand. These studies show preferential binding of Ru(tpy)(dppz)O^{2+} to duplex regions of DNA and semidenatured tRNA and to the bulge site in the TAR DNA. Conversely, new sites were not observed for folded tRNA, which cannot accommodate intercalators. The second set of informative comparisons are to contrast the sites of recognition by Ru(tpy)(dppz)O^{2+} with the sites where the exogenous intercalator Pt(tpy)$(HET)^+$ inhibits oxidation by the nonintercalating Ru(tpy)(bpy)O^{2+} complex. This analysis showed that Pt(tpy)$(HET)^+$ does not perturb the oxidation of folded tRNA by Ru(tpy)(bpy)O^{2+} but does lead to significant changes in the oxidation of the semidenatured form,

(72) Chow, C. S.; Barton, J. K. *Methods Enzymol.* **1992**, *212*, 219−241.
(73) Ghiribi, S.; Maurel, M.-C.; Rougee, M.; Favre, A. *Nucleic Acids Res.* **1988**, *16*, 1095−1112.
(74) Liebman, M.; Rubin, J.; Sundaralingam, M. *Proc. Natl. Acad. Sci. U.S.A.* **1977**, *74*, 4821−4825.
(75) Wells, B. D.; Cantor, C. R. *Nucleic Acids Res.* **1977**, *4*, 1667−1680.
(76) Jones, C. R.; Kearns, D. R. *Biochemistry* **1975**, *14*, 2660−2665.
(77) Ehrenberg, M.; Rigler, R.; Wintermeyer, W. *Biochemistry* **1979**, *18*, 4588−4599.
(78) Tanner, N. K.; Cech, T. R. *Nucleic Acids Res.* **1985**, *13*, 7759−7779.
(79) Weeks, K. M.; Crothers, D. M. *Cell* **1991**, *66*, 577−588.
(80) Delling, U.; Reid, L. S.; Barnett, R. W.; Ma, M. Y.-X.; Climie, S.; Sumner-Smith, M.; Sonenberg, N. *J. Virol.* **1992**, *66*, 3018−3025.
(81) Puglisi, J. D.; Tan, R.; Calnan, B. J.; Frankel, A. D.; Williamson, J. R. *Science* **1992**, *257*, 76−80.

which is consistent with intercalation of $Pt(tpy)(HET)^{+}$ into the semidenatured but not the folded form. The oxidation of the TAR DNA bulge was also inhibited by $Pt(tpy)(HET)^{+}$, again supporting this site as a locus for recognition by intercalators. Thus, the same conclusions are supported by both approaches. The combined results then support strongly the idea that intercalative recognition by the dppz ligand is not just similar to classical intercalators at the level of spectroscopic and physical changes in polymeric DNA but also at the level of single-nucleotide resolution in complex nucleic acid structures.

Acknowledgment. Helpful discussions with Professor T. R. Cech are gratefully acknowledged. This research was supported by the National Science Foundation. H.H.T. acknowledges the support of a Camille Dreyfus Teacher−Scholar Award and an Alfred P. Sloan Fellowship.

Supporting Information Available: Figure S1, HPLC trace showing the formation of 5-methylene-2(5*H*)-furanone in reactions of $Ru(tpy)(dppz)O^{2+}$ with calf thymus DNA; Figure S2, gel showing the cleavage of $tRNA^{Phe}$ by $Ru(tpy)(dppz)O^{2+}$; Figure S3, gel showing inhibition of $Ru(tpy)(bpy)O^{2+}$ cleavage as a result of $Pt(tpy)HET^{+}$ binding to 5′-^{32}P-TAR DNA; and Figure S4, gel showing the effect $Pt(tpy)HET^{+}$ has on the cleavage of 3′-^{32}P-TAR DNA by $Ru(tpy)(bpy)O^{2+}$ (6 pages). See any current masthead page for ordering and Internet access instructions.

JA9729589